Inorganica Chimica Acta xxx (2016) xxx–xxx

Contents lists available at ScienceDirect

Inorganica Chimica Acta

journal homepage: www.elsevier.com/locate/ica

Research paper

Photophysical and bioactivity behavior of *fac*-rhenium(I) derivatives containing ditopic sulfurpyridine ligands

Vanesa Fernández-Moreira *, Héctor Sastre-Martín

Departamento de Química Inorgánica, Instituto de Síntesis Química y Catálisis Homogénea (ISQCH), CSIC-Universidad de Zaragoza, Zaragoza 50009, Spain

ARTICLE INFO

Article history:
Received 21 June 2016
Received in revised form 20 July 2016
Accepted 21 July 2016
Available online xxxx

Keywords:
Rhenium
Thiolate
Thione
Luminescence
Cytotoxicity
Cell imaging

ABSTRACT

Luminescent *fac*-rhenium(I) derivatives have proven their great potential as cell imaging agents. However, there is still a lack of information regarding the structure-bioactivity and biodistribution relationship specially in those cases where the axial ligand is a S-donor ligand. Therefore, new [Re(bipy)$(CO)_3$L]$^{0/+}$ complexes, where L is pyridine-4-thiolate (L1), pyridine-2-thiolate (L2) and 6-methylpyridine-2(1*H*)thione (L3) were synthesised. The ditopic thiol/thione-pyridine derivatives (Spy derivatives) behaved as sulfur donor in all cases, affording two neutral (**1** and **2**) and a cationic (**3**) complex respectively. X-ray diffraction revealed the different coordination mode presented by L2 and L3, a thiolate and a thione donor respectively. Photophysical studies showed that they have moderate emission intensities that are tentatively assigned to ^{3}MLCT transitions (**1**, **2**) and a mixture of ^{1}IL and ^{3}MLCT transition (**3**) with lifetimes in the ns range. Possibly the presence of both, donor and acceptor ligands, SPy and bipyridine respectively, is facilitating a non-radiative LLCT transition to take place, which diminishes the probability of dissipating the energy by a radiative ^{3}MLCT transition. In addition, cytotoxicity assays performed in human cancerous A549 lung and HeLa cervix cells disclosed their poor cytotoxic activity (IC_{50} > 100 μM), which would enable their applications in cell imaging. However, confocal cell microscopy studies performed in A549 cells were not decisive; probably the low emission intensity prevented a clear visualization of the probe.

© 2016 Elsevier B.V. All rights reserved.

1. Introduction

Over the last years, luminescent d^6 metal complexes have been demonstrated to be excellent candidates for cell imaging applications [1,2]. In particular, luminescent Re(I) derivatives with a general formula *fac*-[Re(bisimine)$(CO)_3X]^+$, where X is a pyridine derivative, have attracted great attention in the area due to the easy modulation of their photophysical and biological properties [3,4]. The vast amount of the work reported in this field entails the use of modified pyridine derivatives as the axial N-donor ligands to complete the coordination sphere of the octahedral rhenium complexes [5]. Normally these complexes present well-documented photosphysical properties with emission based in ^{3}MLCT transitions from Re(I) metal centre to the bisimine system. Moreover, they offer good biocompatibility features such as low toxicity, stability under physiological conditions and great capacity to permeate cell membranes [6]. Therefore, elucidating the structure-activity relationship is vital for the further development of specific luminescent probes. Several research groups have been extensively working on this goal. For instance, a mitochondria selective Re(I) probe have been designed by Coogan and coworkers, where a 3-cloromethylpyridine ligand coordinated in the axial position of the {Re(bipy)$(CO)_3$}$^+$ core facilitates its selectivity [7]. The high concentration of thiol groups on the mitochondria and their susceptibility to react with chloromethyl groups induce the probe to get internalized and trapped selectively. Other strategies like the insertion of aminoacid derivatives for easy bio-recognition [8,9], nucleic acid binding groups [10], or biotin structures in the axial pyridine ligand [11] have been also reported, offering a wide variety of possibilities. However, reports on the literature dealing with the luminescent properties of fac-[Re(bisimine)$(CO)_3X]^+$, where X has been substituted for a S-donor derivative, are scarce [12] and those found are limited to the study of their structural properties [13,14]. Additionally, to the best of our knowledge, their application as cell imaging agents has not been explored yet. Therefore, this work expects to engage in the development of luminescent Re(I) thiolate derivatives as cell imaging agents.

* Corresponding author.
E-mail address: vanesa@unizar.es (V. Fernández-Moreira).

http://dx.doi.org/10.1016/j.ica.2016.07.038
0020-1693/© 2016 Elsevier B.V. All rights reserved.

2. Materials and methods

2.1. General measurements and analysis instrumentation

Mass spectra were recorded on a BRUKER ESQUIRE 3000 PLUS, with the electrospray (ESI) technique and on a BRUKER (MALDI-TOF). ^{1}H and $^{13}C\{^{1}H\}$ including 2D experiments, were recorded at room temperature on a BRUKER AVANCE 400 spectrometer (^{1}H, 400 MHz, ^{13}C, 100.6 MHz) with chemical shifts (δ, ppm) reported relative to the solvent peaks of the deuterated solvent. Infrared spectra were recorded in the range 4000–250 cm^{-1} on a Perkin- Elmer Spectrum 100 FTIR spectrometer. Room temperature steady-state emission and excitation spectra were recorded with a Jobin-Yvon-Horiba fluorolog FL3-11 spectrometer fitted with a JY TBX picosecond detection module. UV–vis spectra were recorded with a 1 cm quartz cell on an Evolution 600 spectrophotometer. Lifetimes were measured with a data station HUB-B with a nanoLED controller and DAS6 software. The lifetime data were fitted using the Jobin-Yvon IBH software DAS6 v6.1.

2.2. Crystal structure determinations

Crystals were mounted in inert oil on glass fibers and transferred to the cold gas stream of an Xcalibur Oxford Diffraction diffractometer equipped with a low-temperature attachment. Data were collected using monochromated MoKα radiation (λ = 0.71073 Å). Scan type ω. Absorption corrections based on multiple scans were applied using spherical harmonics implemented in SCALE3 ABSPACK scaling algorithm. The structures were solved by direct methods and refined on F^2 using the program SHELXL-97 [15]. All non-hydrogen atoms were refined anisotropically. Further details on the crystal refinements are collected in Table S1.

2.3. Antoproliferative studies: MTT assay

The MTT assay was used to determine cell viability as an indicator for cells sensitivity to the complexes. Exponentially growing cells were seeded at a density of approximately 10^4 cells per well in 96-well flat-bottomed microplates and allowed to attach for 24 h prior to addition of compounds. The complexes were dissolved in DMSO and added to cells in concentrations ranging from 2.5 to 100 μM in quadruplicate. Cells were incubated with our compounds for 24 h at 37 °C. Ten microliters of MTT (5 mg ml^{-1}) were added to each well and plates were incubated for 2 h at 37 °C. Finally, plates were centrifuged for 10 min at 500×g, media was eliminated and DMSO (100 ml per well) was added to dissolve the formazan precipitates. The optical density was measured at 550 nm using a 96-well multiscanner autoreader (ELISA). The IC_{50} was calculated by nonlinear regression analysis.

2.4. Cell fluorescence microscopy study

European Collection of Cell Cultures, were maintained in Hepes modified minimum essential medium (HMEM) supplemented with 10% fetal bovine serum, penicillin, and streptomycin. Cells were detached from the plastic flask using trypsin-EDTA solution and suspended in an excess volume of growth medium. The homogeneous cell suspension was then distributed into 30 μl aliquots in a 6 channel μ-slide IV0.4 (IBIDI), with each aliquot being subject to incubation with the different complexes, final concentrations of 100 μM, at 37 °C for 24 h. Then, 30 μl of a solution 5 μM the internal standard (DRAQ5) in cell growth medium was added to each well. Preparations were viewed using an Olympus FV10-i Oil type compact confocal laser microscope using an ×10 or ×60 objective, with excitation wavelength at 405, 473 and 650 nm.

2.5. Materials and procedures

The intermediate fac-[Re(bipy)$(CO)_3(CF_3SO_3)$] was prepared according to literature procedures [16]. All other starting materials and solvents were purchased from commercial suppliers and used as received unless otherwise stated.

3. Experimental

3.1. Complex **1**

An excess of pyridine-4-thiolate (100 mg, 0.900 mmol) was added to a solution of [Re(bipy)$(CO)_3(CF_3SO_3)$] (78 mg, 0.136 mmol) in dry CH_2Cl_2 (20 mL). The mixture was stirred for 48 h at room temperature under an argon atmosphere. Then, 2/3 of the solvent was removed under vacuum to afford a yellow solid, which was filtered and further washed with ether. Complex **1** was obtained as a yellow solid after purification by column cromatography in alumina gel using a mixture of CH_2Cl_2: methanol (70:1) and gradually increasing its polarity. (43 mg, 59%). ^{1}H NMR (400 MHz, $(CD_3)_2CO$) δ 9.06 (d, J = 5.5 Hz, 2H, CH(6, 6′) bipy), 8.61 (d, J = 7.9 Hz, 2H, CH(3, 3′) bipy), 8.28 (td, J = 7.9, 1.5 Hz, 2H, CH (4, 4′) bipy), 7.85 (dd, J = 4.7, 1.4 Hz, 2H, CH(2, 6) py), 7.75 (ddd, J = 7.9, 5.5, 1.2 Hz, 2H, CH(5, 5′) bipy), 6.89 (dd, 4.7, 1.4 Hz, 2H, CH(3, 5) py). ^{13}C NMR (101 MHz, $(CD_3)_2CO$) δ 158.2 ((C(4) py)), 156.2 ((C(2, 2′) bipy)), 154.0 ((C(6, 6′) bipy)), 148.5 ((C(2, 6) py)), 140.4 ((C(4, 4′) bipy)), 129.5 ((C(3, 5) py)), 128.5 ((C(5, 5′) bipy)), 124.9 ((C(3, 3′) bipy)). IR (sol, cm^{-1}, ν(CO)): 2005, 1901, 1877. MS $(ESI)^+$: m/z 538.1 ($[MH]^+$, 100%), calculated 538.0.

3.2. Complex **2**

This compound was prepared similarly to **1** using pyridine-2-thiolate instead of pyridine-4-thiolate. The product obtained was a yellow solid (67 mg, 92%). ^{1}H NMR (400 MHz, $(CD_3)_2CO$) δ 9.18 (dt, J = 5.5, 1.1 Hz, 2H, CH(6, 6′) bipy), 8.59 (d, J = 7.9 Hz, 2H, CH(3, 3′) bipy), 8.22 (td, J = 7.9, 1.1 Hz, 2H, CH(4, 4′) bipy), 8.04 (ddd, J = 4.9, 1.9, 1.0 Hz, 1H, CH(6) py), 7.68 (ddd, J = 7.9, 5.5, 1.0 Hz, 2H, CH(5, 5′) bipy), 7.02 (ddd, J = 7.9, 7.2, 1.9 Hz, 1H, CH(4) py), 6.93 (dt, J = 7.9, 1.0 Hz, 1H, CH(3) py), 6.62 (ddd, J = 7.2, 4.9, 1.0 Hz, 1H, CH(5) py). ^{13}C NMR (101 MHz, $(CD_3)_2CO$) δ 169.8 (C(2) py), 156.6 (C(2, 2′) bipy), 154.7 (C(6, 6′) bipy), 148.5 (C(6) py), 140.0 (C(4, 4′) bipy), 134.4 (C(4) py), 127.5 (C(5, 5′) bipy), 126.8 (C(3) py), 124.5 (C(3, 3′) bipy), 117.0 (C(5) py). IR (sol, cm^{-1}, ν(CO)): 2002, 1878. MS $(ESI)^+$: m/z 538.1 ($[MH]^+$, 100%), calculated 538.0.

3.3. Complex **3**

This compound was prepared similarly to **1** using 6-methylpyridine-2(1*H*)thione instead of pyridine-4-thiolate and increasing the reaction time from 48 to 96 h. Purification was performed by recrystallization from CH_2Cl_2. The product obtained was an orange solid (85 mg, 70%). ^{1}H NMR (400 MHz, $(CD_3)_2CO$) δ 12.18 (s, 1H, NH py), 9.15 (ddd, J = 5.5, 1.6, 1.0 Hz, 2H, CH(6, 6′) bipy), 8.76 (dt, J = 8.2, 1.0 Hz, 2H, CH(3, 3′) bipy), 8.41 (ddd, J = 8.2, 7.7, 1.6 Hz, 2H, CH(4, 4′) bipy), 7.94 (t, J = 7.9 Hz, 1H, CH(4) py), 7.86 (ddd, J = 7.6, 5.5, 1.0 Hz, 2H, CH(5, 5′) bipy), 7.49 (d, J = 7.9 Hz, 1H, CH (5) py), 7.29 (d, J = 7.9 Hz, 1H, CH(3) py), 2.55 (s, 3H, CH_3 py). ^{13}C NMR (101 MHz, $(CD_3)_2CO$) δ 197.9 (CO), 190.3 (CO), 167.4 (C(2) py), 156.4 (C(2, 2′) bipy), 154.4 (C(6, 6′) bipy), 153.9 (C(6) py), 144.2 (C(4) py), 141.4 (C(4, 4′) bipy), 130.4 (C(5) py), 129.1 (C(5, 5′) bipy), 125.5 (C(3, 3′) bipy), 121.0 (C(3) py), 19.3 (C(CH_3) py). IR (sol, cm^{-1}, ν(CO)): 2035, 2023, 1915, 1886. MS $(ESI)^+$: m/z 552.1 ($[MH]^+$, 100%), calculated 552.0.

Please cite this article in press as: V. Fernández-Moreira, H. Sastre-Martín, Inorg. Chim. Acta (2016), http://dx.doi.org/10.1016/j.ica.2016.07.038

4. Results and discussion

4.1. Synthesis and characterization

Complexes *fac*-[Re(bipy)$(CO)_3$L]$^{0/+}$ (**1–3**), where L represents a ditopic thiol/thione pyridine derivative (Spy), specifically pyridine-4-thiolate (L1), pyridine-2-thiolate (L2) and 6-methylpyridine-2(1*H*)thione (L3) respectively, were synthesised following the standard synthetic route for these type of octahedral rhenium(I) complexes [16–19]. Specifically, the synthesis involved the initial formation of *fac*-[Re(bipy)$(CO)_3$Cl], then activation of the species by exchange of the chloride to a triflate, and finally, the substitution of the triflate by the ditopic Spy derivative affording the corresponding rhenium(I) complexes (**1–3**), see Fig. 1.

Spectroscopic characterization was performed by FTIR, ^{1}H and ^{13}C NMR and two dimensional NMR experiments to ascertain the assignment. Moreover, further analytical data provided by electrospray ionization mass spectroscopy (ESI-MS) corroborated the success on the synthesis. Additionally, crystalline structures of complexes **2** and **3** have been solved by X-ray analysis. Specifically, IR spectroscopy revealed a different coordination mode of the Spy derivatives for complexes **1–3**. Thus, the Spy derivative behaves as a thiolate donor in the case of complex **1** and **2** and as a thione donor for complex **3,** affording two neutral complexes and a cationic complex respectively. As expected, the strong υ(CO) stretching bands in the range of 2005 and 1877 cm^{-1} seen for the neutral species are shifted to 2035–1886 cm^{-1} in the case of complex **3** corroborating its cationic nature [17]. Moreover, the shift of υ(C-S) stretching band of complexes **1** and **2** from c.a. 757 cm^{-1} to 767 cm^{-1} in complex **3** is in agreement with the thione character played by L3, Table 1, [20]. Further ^{1}H NMR spectroscopy analysis agrees with this result. The most relevant difference between the chemical shifts of these species relays in the bipyridine proton C*H*(4) that feels a higher deshielding in the case of complex **3** than the analogous protons in the neutral species **1** and **2**. Specifically proton C*H*(4) appears at 8.41 ppm in complex **3** whereas at 8.28 and 8.22 ppm in complexes **1** and **2** respectively. In addition to that, a NH proton peak is present at 12.18 ppm in complex **3**. Moreover, the facial disposition of the CO ligands is validated by the four set of protons and carbons corresponding to the bipyridine ligand seen in the ^{1}H and ^{13}C NMR spectra implying the presence of a symmetry plane within the molecule [21]. Thiol/thione-pyridine derivatives present a tautomeric equilibrium, normally displaced towards the thione from [22]. The fact that L3 has a methyl group as substituent, which is an electron donor group by inductive effect, probably displaces the equilibrium even more towards the thione form. Therefore, it is not surprising that L2 and L3 displayed a different coordination mode, with L3 preferring the thione form.

Table 1
Relevant IR stretching frequencies, ^{1}H chemical shifts and [MH$^+$] values.

Complex	υ(CO)/cm^{-1}	CH(4)bipy/ppm	NH/ppm	ESI-MS
1	2005, 1901, 1877	8.28	–	538.1
2	2002, 1878	8.22	–	538.1
3	2035, 2023, 1915, 1886	8.41	12.18	552.1

4.2. X-ray crystallograpy

Single crystals suitable for X-ray diffraction analysis of complexes **2** and **3** were obtained by slow diffusion of hexane into a CH_2Cl_2 solution. Relevant crystallographic data are reported in Tables S1–S3. The coordination sphere of both complexes can be described as a distorted octahedron where the three carbonyls are arranged in a facial disposition. Hence, in both cases, the bipyridine ligand and two carbonyl ligands are situated in the equatorial plane and the third carbonyl and the Spy derivative are in the axial position. Complex **2** crystalized in a monoclinic C2/c space group whereas complex **3** in monoclinic Pn. Both of them display a single molecule per asymmetric unit and bond distances around the metal centre do not differ from those reported previously for similar complexes [23]. Thus, Re–C(CO) distances are between 1.908 (4) and 1.931(3) Å and Re–N(bipy) between 2.166(3) and 2.181 (4) Å. Similarly, angles within the coordination sphere of both species are alike, being N(1)Re(1)N(2), at 74.92(15) and 72.82(9)° respectively for each molecule, the source for the deviation from the ideal octahedral geometry. In concordance with the spectroscopic experimental data seen so far for complexes **2** and **3**, the main difference between the crystalline structure of both complexes is based on the coordination mode presented by the Spy derivative. In both cases the Spy binds the metal centre through the sulfur atom, but, as a thiolate in the case of complex **2** and as a thione for complex **3**. Consequently, Re-S distances and Re-S-C angles of both species differ considerably, ie. Re(1)-S(1) bond distances of 2.4945(13) and 2.5428(10) Å and Re(1)-S(1)-C(14) angles of 112.17(19) and 104.85(10)° respectively. In addition, in complex **2**, the angle between the planes containing the L2 ring, specifically the plane described by the atoms (C15C14N3), with th e plane formed by the two nitrogens of the bypiridine system and one carbon atom of a carbonyl ligand, (N1N2C1), is 84.93°, implying their almost perpendicular disposition. However, the same angle for complex **3** is only 16.49°, leaving the Spy ring nearly parallel with the bipyridine system, Fig. S1. Therefore, π-π stacking could be considered between L3 and one of the pyridine ring of the bipyridine system, see Fig. 2, [24]. Moreover, the proton H(3), the nitrogen proton of L3 in complex **3**, establishes a hydrogen bond with an oxygen atom of the counter ion, H(3)...O(4) of 1.77(4) Å, see Fig. 2. Alternatively, complex **2** presents a close contact inter-

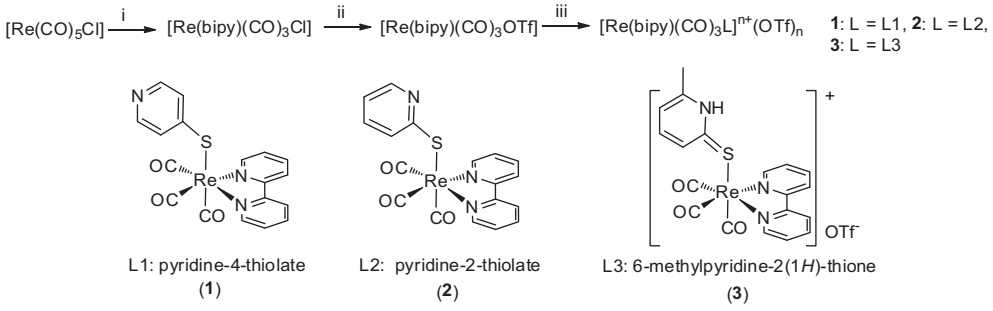

Fig. 1. Depiction of the synthesis of complexes **1**, **2** and **3**. Reaction conditions: (i) bipy, toluene, reflux, 1 h; (ii) CF_3SO_3H, CH_2Cl_2, rt, 45 min; (iii) L1, L2 or L3, CH_2Cl_2, rt, 48 h.

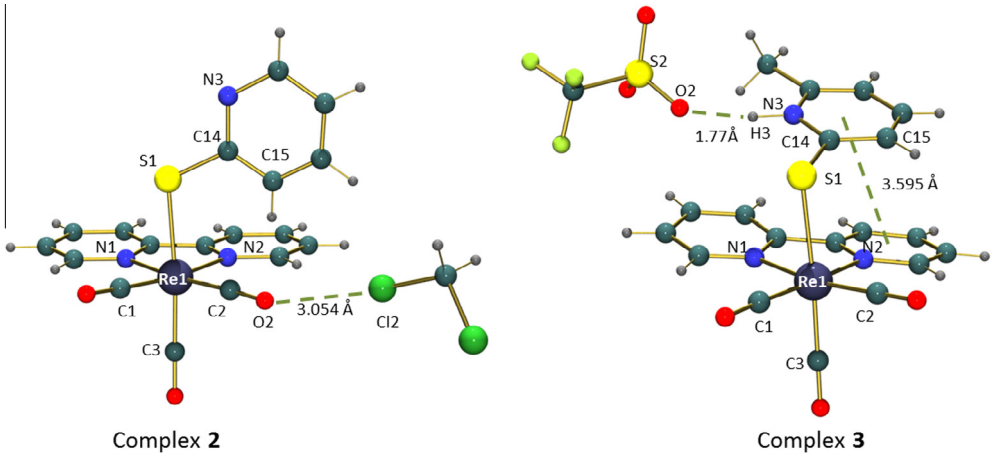

Fig. 2. Ortep representation of complex **2** and **3**. The most relevant bond lengths (Å) and angles (deg): Complex 2: Re(1)-C(1) = 1.917(5), Re(1)-C(2) = 1.917(6), Re(1)-C(3) = 1.924(6), Re(1)-N(1) = 2.181(4), Re(1)-N(2) = 2.170(4), Re(1)-S(1) = 2.4945(13); N(1)-Re(1)-N(2) = 74.92(15), C(3)-Re(1)-S(1) = 175.12(17); Complex 3: Re(1)-C(1) = 1.908 (4), Re(1)-C(2) = 1.925(3), Re(1)-C(3) = 1.931(3), Re(1)-N(1) = 2.166(3), Re(1)-N(2) = 2.174(3), Re(1)-S(1) = 2.5428(10); N(1)-Re(1)-N(2) = 74.82(9), C(3)-Re(1)-S(1) = 176.31 (10).

action between the oxygen O(2) of one of the carbonyl ligands with a chloride atom from a dichlomethane molecule present as a crystallization solvent molecule, i.e. Cl(2)...O(2) = 3.054(4) Å.

4.3. Photophysical studies

The electronic UV-spectra of complexes **1–3** were recorded in CH_2Cl_2 solution and showed the typical absorption pattern associated with bisimine Re(I) derivatives, i.e. ligand-centred transitions (bipyridine, Spy) at higher energy and metal to ligand charge-transfer transitions (^{1}MLCT) at lower energy. Relevant absorption data are collected in Table 2.

Specifically, the UV-absorption spectrum patterns of complex **1** and **2** are alike, with two intense bands centred at c.a. 245 and 290 nm that are attributable to the spin allowed intraligand, ^{1}IL, transition, $\pi \rightarrow \pi^*$ and $n \rightarrow \pi^*$ respectively, within the aromatic ligands and a much less energetic band at c.a. 480 nm that was tentatively assigned to a metal-to-ligand-charge-transfer, ^{1}MLCT, transition, i.e. a $Re(d\pi) \rightarrow bipy(\pi^*)$ transition [25]. Alternatively, complex **3** also presented three intense absorption bands at 241, 288 and 377 nm that were assigned to ^{1}IL transitions $\pi \rightarrow \pi^*$ and $n \rightarrow \pi^*$ among the bipy and Spy ligand [26,27]. The MLCT transition was not clearly observed in this case. Probably the highly intense IL transition at 377 nm that exhibits a tail reaching up to 450 nm is disguising the expected transition, Fig. 3.

Emission and excitation spectra of **1**, **2** and **3** were measured in CH_2Cl_2 solution at 298 K, Fig. 4, exhibiting an extremely low emission and absorption intensity in comparison with their analogue *fac*-[Re(bipy)$(CO)_3$X] complexes, where X is a N-donor pyridine derivative. Once more, complexes **1** and **2** displayed a similar emission pattern. Both of them presented a broad structureless emission band centred at 572 and 675 nm respectively that could be assigned to a ^{3}MLCT transition [12]. Instead, complex **3** presented two emissions bands with a different profile, i.e. a sharp highly intense emission at 545 nm and a moderately intense broad emission at 679 nm.

The least energetic emission band centred at 679 nm resembles the emission pattern seen for the analogous complex **2**, therefore the same ^{3}MLCT transition assignation is proposed. As commented, the emission intensity observed for the ^{3}MLCT transition of **1–3** was relatively low in comparison with this of their parent *fac*-[Re(bipy)$(CO)_3$X] complexes, where X is a N-donor pyridine derivative. Therefore, a secondary process might be dissipating the energy in a non-radiative pathway. K.S. Schanze and coworkers have suggested the presence of a ligand-to-ligand-charge-transfer, LLCT, transition as an alternative pathway in those d^6 transition metal complexes containing electron donor and electron acceptor ligands [28]. In the present case, Spy and biyridine ligands could be behaving as such, promoting electrons from Spy to the biyridine ligand in the excited states. Despite their poor electronic interaction, it is possible to populate the LLCT state by a combination of an MLCT transition followed by a fast forward intramolecular electron transfer process, see Fig. 5. Generally, LLCT decay occurs primarily via non-radiative back energy transfer transition, BET, which is competition with the radiative decay of ^{3}MLCT excited state, and possibly causing the low intensity emission observed experimentally for complexes **1–3**.

In addition, the red shift on the MLCT emission observed for complexes **2** and **3** in comparison with **1** could be explained in terms of the different π-donation character of 4-Spy and 2-Spy derivatives. Better π-donor ligands make the metal centre richer in electrons and more susceptible to oxidization, which reduces the MLCT energy by destabilization of the HOMO orbitals and consequently the emission maximum shifts from 572 to ca. 675 nm [29]. An alternative explanation ought to be given for the sharp emission band present at 545 nm in complex **3**. Considering the structural difference between the synthesised complexes, it seems clear that the protonated pyridine-thione L3 is displaying an additional emission band. Fig. 6 shows the emission and excitation spectra upon exciting at 450 and at 520 nm revealing two different electronic transitions, ie. a MLCT and a ILCT transition respectively. Similarly, Pilato and coworkers have reported the luminescence studies for neutral and cationic Pt(II) complexes containing a

Table 2
Photophysical data of complexes **1–3**.

	Absorption[1]/nm (ε/$M^{-1}Cm^{-1}$)	Emission[1]/nm (Excitation[1]/nm)	τ/ns
1	249 (17300), 295 (11100), 369 (2560), 488 (420)	572(432)	120
2	245 (15100), 284 (13000), 353 (2870), 494, (470)	675(425)	48
3	241 (21500), 288 (21800), 374 (15700)	679(472) 545(522)	47 140

[1] CH_2Cl_2 solution at 298 K.

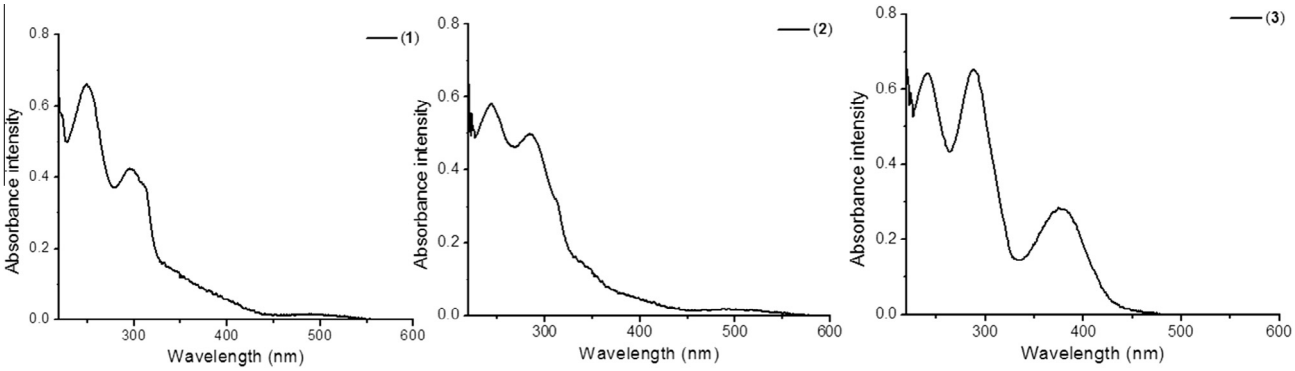

Fig. 3. UV-absorption spectra of complexes **1**, **2** and **3**.

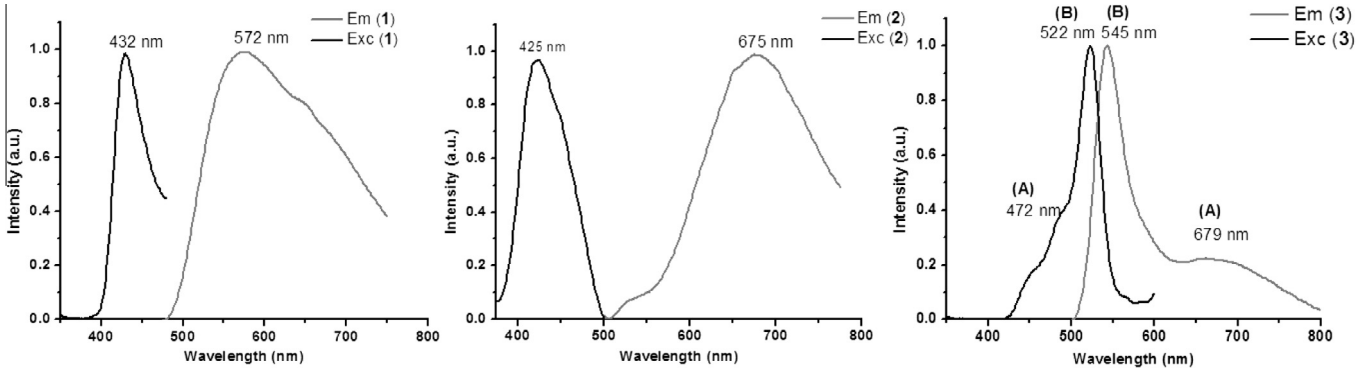

Fig. 4. Excitation and emission spectra of complexes **1** (λ_{exc} = 430 nm), **2** (λ_{exc} = 425 nm) and **3** (λ_{exc} = 475 nm).

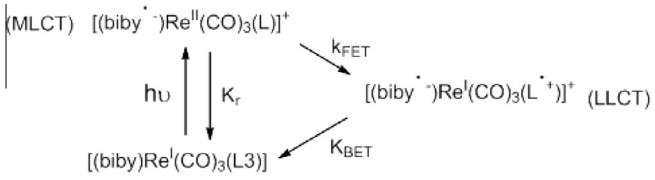

Fig. 5. Proposed photophysical process for MLCT and LLCT transitions.

pyridine and a protonated pyridine as substituents of the dithiolene ligand used as chelator. Their findings demonstrate that upon protonation of the pyridine, ^{1}ILCT and ^{3}ILCT excited state drop substantially in energy allowing for efficient fluorescence and phosphorescence [30,31]. Consequently, the emission band centred at 545 nm, seen only in the case of complex **3** where the axial ligand is the pyridine-2(1H)-thione tautomer, could assigned to the ILCT transition within the protonated sulfur-pyridine derivative. Lifetime of complexes **1–3** was also measured in CH_2Cl_2 solution, giving values of 120, 48 and 47 ns respectively and agreeing with the ^{3}MLCT assignation [29]. Additionally, the high energy band observed in complex **3** initially assigned to ILCT, presented a lifetime value of 140 ns. This result together with the small Stokes shift observed for this transition, might suggest that it is a fluorescence process the one that takes place, i.e. a ^{1}ILCT transition.

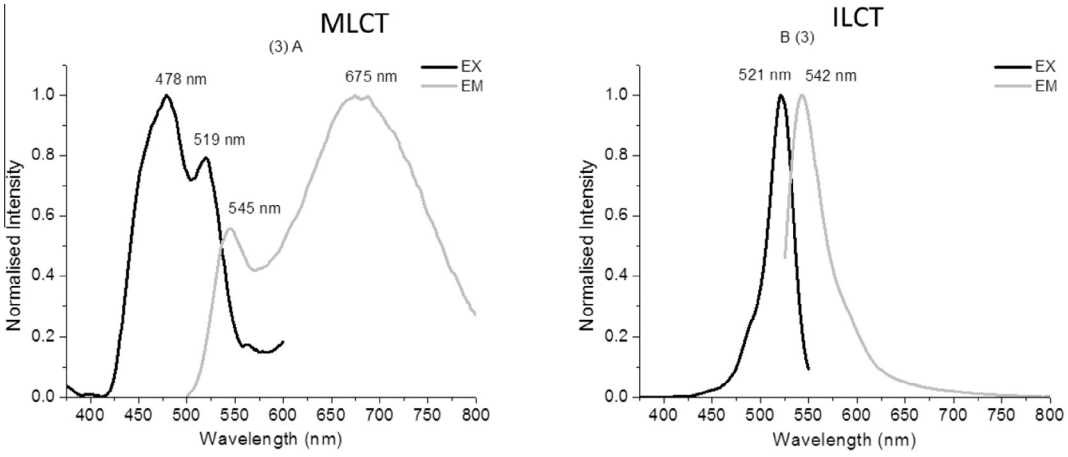

Fig. 6. Emission and excitation spectra of complex **3** exhibiting the ^{3}MLCT and ^{1}ILCT transitions. λ exc = 450 nm (left), λ exc = 520 nm (right).

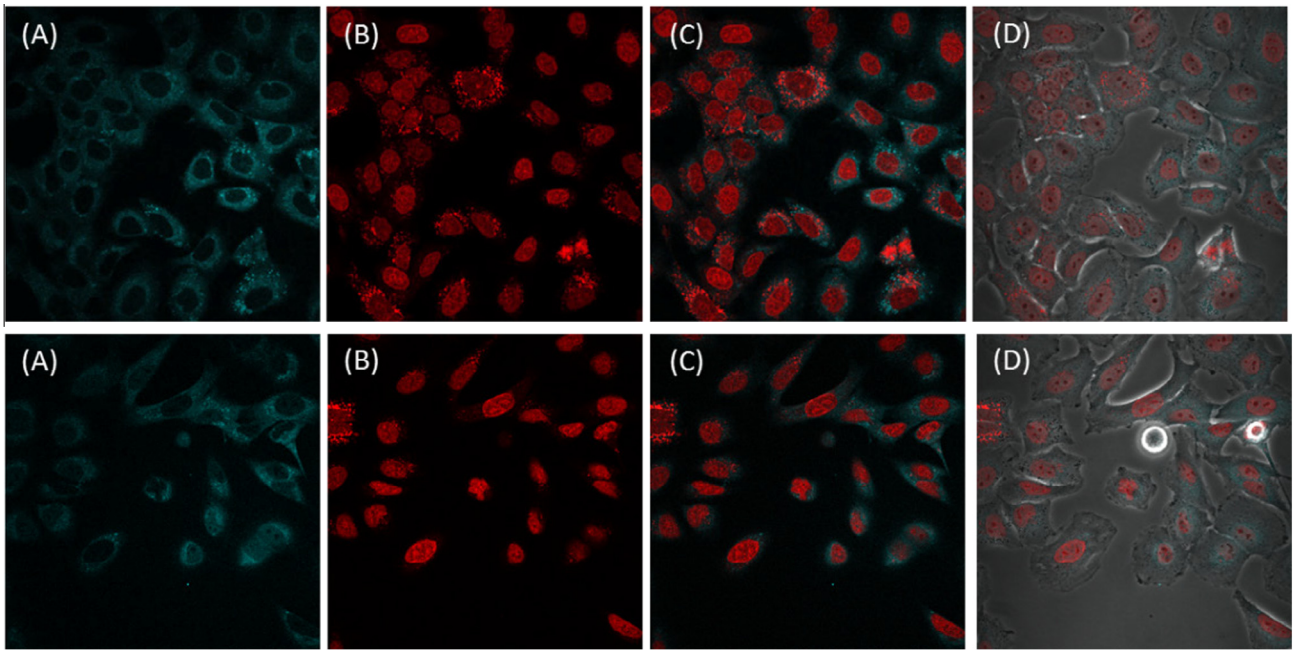

Fig. 7. Fluorescence cell images of A549 cell incubated with complex **2** at 100 μM and DRAQ5 for 24 h (first row) and with no complex (second row). (A) Images upon irradiation at 405 nm to visualize complex **2**. (B) Images upon irradiation at 650 nm to visualize the internal standard DRAQ5. (C) Superimposition image of A and B. (D) Superimposition image of A, B and the bright field.

4.4. Antiproliferative studies and fluorecence microcopy

The antiproliferative activity of complexes **1–3** in cancerous cells was determined by an MTT assay. Thus, the synthesised complexes were incubated with cervix (HeLa) and lung (A549) carcinoma cell lines for 24 h. As expected, none of them showed any cytotoxicity at the measured concentration, $IC_{50} > 100$ μM, see Table 3, which inspired their use in fluorescence cell microscopy as cell imaging agents [32]. Many research groups have already tested the capacity as cell imaging agent for *fac*-[Re(bipy)$(CO)_3X]^+$, where X is a pyridine derivative, however, no reports have been published where X is a sulfur donor derivative [8,33]. Consequently, fluorescence cell microscopy was used to ascertain their possible cellular biodistribution and localization. Complexes **1–3** were incubated for 24 h in A549 lung carcinoma cells using loading concentrations of 100 μM, i.e. concentration below their IC_{50} to prevent cellular death. Moreover, DRAQ5, a commercial nuclear dye, was used as internal standard. Confocal fluorescent images were taken after excitation at either 405 or 473 nm, to visualize the synthesised complexes, and at 655 nm for the visualization of the commercial fluorophore. Unfortunately, comparison between the images obtained for the cells incubated with the complexes and the control, i.e. neat cells, did not draw any clear conclusion. Fig. 7 shows as the cells incubated with complex **2** displayed a granular emission in the cytoplasm area, which could be considered mitochondrial localization by comparison with published report on similar complexes [7,34,35]. However, an analogous granular distribution was seen for the control cells when they were irradiated at 405 nm revealing the possible interference of the cells autofluorescence. Although, such blue emission seems to be stronger in the case of the complex **2**, the intensity emission differences in the row images are too subtle to be able to claim such localization. The same result was obtained for complexes **1** and **3**, see Fig. S2. Possibly, the low emission intensity already observed for those complexes during their photophysical study is preventing to visualize their biodistribution.

Table 3
IC_{50} values for complexes **1–3** in HeLa and A549 cells.

Complex	IC_{50} (Hela)[1]	IC_{50}(A549)[1]
1	>100	>100
2	>100	>100
3	>100	>100

[1] Values after 24 h incubation (μM).

5. Conclusions

In summary, we have reported the synthesis of three novel *fac*-[Re(bipy)$(CO)_3L]^{0/+}$ derivatives where L is either a pyridine-4-thiolate, a pyridine-2-thiolate or a 6-methylpyridine-2(1*H*)thione affording two neutral (**1**, **2**) and a cationic (**3**) complex. Although the Spy ligands offer two coordination sites possibilities, i.e. N-donor or S-donor, the metal centre binded preferably through the sulfur atom. Moreover, spectroscopy characterization and X-ray diffraction apart from confirming the expected octahedral disposition of the ligands around the metal centre, revealed the different coordination mode presented by L2 and L3, a thiolate and a thione donor respectively. Luminescence studies showed the typical broad emission band centred at 572 nm for complex **1** and at c.a. 675 for complex **2** and **3** that was assigned to ^{3}MLCT transitions. Emission intensity for these transitions are relatively lower than this of analogous *fac*-[Re(bipy)$(CO)_3L]^{0/+}$, where L is a N-donor pyridine derivative. Possibly the presence of both, donor and acceptor ligands, is facilitating a LLCT transition from the Spy derivative to the bipy ligand to take place. Thus, competition between the non-radiative LLCT and the MLCT transition diminishes the probability of the latter to occur and consequently its emission intensity is considerably reduced. Additionally complex **3** presented an intense, sharp emission band at 545 nm that was tentatively attributable to a ^{1}IL transition within the and 6-methylpyridine-2(1*H*) thione. None of the complexes presented any cytotoxicity at the measured concentration in tumor HeLa and A549 cells. Confocal cell microscopy studies performed in A549 cell showed a faint granular emission in the cytoplasm area which could be considered mitochondrial localization. Nevertheless this result was not conclusive because of the low emission intensity of the probes and

the possible presence of autofluorescence. Therefore, although *fac*-$[Re(bipy)(CO)_3L]^{0/+}$, where L is a pyridine derivative, have shown to be excellent cell imaging agents, this capacity is lost when the pyridine is substituted by a Spy and the preferred coordination site is thought the sulfur atom.

Author contributions

The synthesis and spectroscopic characterization of the complex **1** and **2** were carried out by Vanesa Fernández-Moreira and this of complex **3** by Héctor Sastre Martín. Photophysical and fluorescence microscopy studies were performed by Vanesa Fernández-Moreira and the antiproliferative assays were executed by both authors. Data analysis and preparation of the manuscript were performed by vanesa Fernández-Moreira.

Conflicts of interest

The authors declare no conflict of interest.

Acknowledgments

Authors thank the Ministerio de Economía y Competitividad (MINECO-FEDER CTQ2013-48635-C2-1-P, and CTQ2015-70371-REDT) and Gobierno de Aragón-Fondo Social Europeo (E77) for financial support. V.F-M thanks Prof. M.C. Gimeno for measuring and solving the crystalline structures and her unconditional support and Prof. A. Laguna for his recommendation to participate in this special issue.

Appendix A. Supplementary data

Crystal data and structure refinement for compounds **2** and **3.** Fluorescence cell images. CCDC 1482274 and 1482275 contain the supplementary crystallographic data for **2** and **3**. Supplementary data associated with this article can be found, in the online version, at http://dx.doi.org/10.1016/j.ica.2016.07.038.

References

[1] M.P. Coogan, V. Fernández-Moreira, Chem. Commun. 50 (2014) 384.
[2] K.K.-W. Lo, Acc. Chem. Res. 48 (2015) 2985.
[3] V. Fernández-Moreira, F.L. Thorp-Greenwood, A.J. Amoroso, J. Cable, J.B. Court, V. Gray, A.J. Hayes, R.L. Jenkins, B.M. Kariuki, D. Lloyd, C.O. Millet, C.F. Williams, M.P. Coogan, Org. Biomol. Chem. 8 (2010) 3888.
[4] A. Kumar, S.-S. Sun, A.-L. Lees, Top. Organomet. Chem. 29 (2010) 1.
[5] K.K.-W. Lo, K.Y. Zhang, S.P.-Y. Li, Eur. J. Inorg. Chem. (2011) 3551.
[6] D.-L. Ma, C.-M. Che, F.-M. Siu, M. Yang, K.-Y. Wong, Inorg. Chem. 46 (2007) 740.
[7] A.J. Amoroso, R.J. Arthur, M.P. Coogan, J.B. Court, V. Fernández-Moreira, A.J. Hayes, D. Lloyd, C. Millet, S.J.A. Pope, New J. Chem. 32 (2008) 1097.
[8] V. Fernández-Moreira, M.L. Ortego, C.F. Williams, M.P. Coogan, M.D. Villacampa, M.C. Gimeno, Organometallics 31 (2012) 5950.
[9] S.Y. Reece, D.G. Nocera, J. Am. Chem. Soc. 127 (2005) 9448.
[10] L. Wei, J. Babich, W.C. Eckelman, J. Zubieta, Inorg. Chem. 44 (2005) 2198.
[11] K.K.-W. Lo, M.-W. Louie, K.-S. Sze, J.S.-Y. Lau, Inorg. Chem. 47 (2008) 602.
[12] V.W.-W. Yam, K.M.-C. Wong, K.-K. Cheung, Organometallics 16 (1997) 1729.
[13] D.J. Kramer, A. Davison, W.M. Davis, A.G. Jones, Inorg. Chem. 41 (2002) 6181.
[14] E. Hevia, J. Pérez, V. Riera, Organometallics 21 (2002) 5312.
[15] G.M. Sheldrick, Acta Crystallogr. A 64 (2008) 112.
[16] J.K. Hino, L.D. Ciana, W.J. Dressick, B.P. Sullivan, Inorg. Chem. 31 (1992) 1072.
[17] J.V. Caspar, T.J. Meyer, J. Phys. Chem. 87 (1983) 952.
[18] Y. Wang, L.A. Lucia, K.S. Schanze, J. Phys. Chem. 99 (1995) 1961.
[19] A.J. Amoroso, M.P. Coogan, J.E. Dunne, V. Fernández-Moreira, J.B. Hess, A.J. Hayes, D. Lloyd, C. Millet, S.J.A. Pope, C. Williams, Chem. Commun. (2007) 3066.
[20] F. Grifasi, M.R. Chierotti, C. Garino, R. Gobetto, E. Priola, E. Diana, F. Turci, Cryst. Growth Des. 15 (2015) 2929.
[21] S.V. Wallendael, R.J. Shaver, D.P. Rillema, B.J. Yoblinski, M. Stathis, T.F. Guarr, Inorg. Chem. 29 (1990) 1761.
[22] B.P. Kennedy, A.B.P. Lever, Can. J. Chem. 50 (1972) 3488.
[23] A. Casula, V. Nairi, V. Fernández-Moreira, A. Laguna, V. Lippolis, A. Garau, M.C. Gimeno, Dalton Trans. 44 (2015) 18506.
[24] C.A. Janiak, J. Chem. Soc. Dalton Trans. (2000) 3885.
[25] Y. Kim, F.W.M. Vanhelmont, C.L. Stern, J.T. Hupp, Inorg. Chim. Acta 318 (2001) 53.
[26] P. Beak, F.S. Fry Jr., J. Lee, F. Steele, J. Am. Chem. Soc. 98 (1976) 171.
[27] R. Du, C. Liu, Y. Zhao, K.-M. Pei, H.-G. Wang, X. Zheng, M. Li, J. Phys. Chem. B 115 (2011) 8266.
[28] Y. Wang, B.T. Hauser, M.M. Rooney, R.D. Burton, K.S. Schanz, J. Am. Chem. Soc. 115 (1993) 5675.
[29] L.A. Sacksteder, A.P. Zipp, E.A. Brown, J. Streich, J.N. Demas, B.A. DeGraff, Inorg. Chem. 29 (1990) 4335.
[30] S.P. Kaiwar, A. Vodacek, N.V. Blough, R.S. Pilato, J. Am. Chem. Soc. 119 (1997) 9211.
[31] S.P. Kaiwar, A. Vodacek, N.V. Blough, R.S. Pilato, J. Am. Chem. Soc. 119 (1997) 3311.
[32] V. Fernández-Moreira, I. Marzo, M.C. Gimeno, Chem. Sci. 5 (2014) 4434.
[33] K.Y. Zhang, K.K.-S. Tso, M.-W. Louie, H.-W. Liu, K.K.-W. Lo, Organometallics 32 (2013) 5098.
[34] S. Imstepf, V. Pierroz, R. Rubbiani, M. Felber, T. Fox, G. Gasser, R. Alberto, Angew. Chem. Int. Ed. 55 (2016) 2792.
[35] E.E. Langdon-Jones, N.O. Symonds, S.E. Yates, A.J. Hayes, D. Lloyd, R. Williams, S.J. Coles, P.N. Horton, S.J.A. Pope, Inorg. Chem. 53 (2014) 3788.